ADJUSTMENT OF A DOUBLE DRIFT HARMONIC BUNCHER AND BUNCH SHAPE MEASUREMENTS

J. Knott, D. Warner and M. Weiss
CERN, Geneva, Switzerland

Summary

The longitudinal beam matching of the new 50 MeV linac is achieved with a double drift harmonic buncher. For optimum bunching efficiency the RF phase difference between the two cavities should be known and controlled to about 1° (at 202.56 MHz). The adjustment of the RF levels and phases is based on observations of the bunch form via a broad-band probe connected to a travelling wave oscilloscope. The time base is tightly locked to the RF by a specially developed circuit allowing a systematic study of different bunching conditions. A comparison is made between some preliminary measurements and the waveforms predicted by a simplified theory.

Introduction

The aim of a linac bunching system is to produce, via modulation of the proton beam prior to its injection, bunches which will be matched to the longitudinal phase plane acceptance of the accelerator. These bunches will remain stable if their space charge density distribution is compatible with the available longitudinal focusing arising from the acceleration process. To have a good control of the filling of the longitudinal acceptance, a bunching system containing a double drift harmonic buncher (DDHB) has been chosen for the CERN new 50 MeV linac[1] (see Fig. 1). Such a buncher works efficiently only if the RF voltages on the gaps of the first and second harmonic cavities are adjusted correctly, a particularly important parameter being their respective phases (precision of the order of 1-2° at 200 MHz).

This paper treats the problem of the correct adjustment of the DDHB by bunch shape measurements. The approach is essentially the same as the one applied for a single buncher[2]. A coaxial probe detects the bunch density in a destructive manner, and the broad-band signal is transmitted via a matched circuit to a display device, a high-speed oscilloscope. Improvements have been achieved in the construction of the broad-band probe following the suggestions outlined in Ref. 2, and new electronic circuitry has been developed[3], permitting a tight locking of the horizontal sweep of the oscilloscope with the phase of the RF frequency (200 MHz). This last point was essential for obtaining a clear picture on the oscilloscope screen (real-time measurement).

The experiments reported here were done at 500 keV with a double buncher and sufficient focusing before the probe to obtain a realistic approximation to an actual linac bunching system[3] (Fig. 1). Note that on the new linac the beam energy will be 750 keV, the focusing system much more complex (six quadrupoles), and the final longitudinal matching will use an energy correction cavity placed 165 mm before the first linac accelerating gap[1]. In comparison with previous studies the emphasis here is on effects peculiar to double buncher systems. Thus the simplified theory shows the dependence of bunching on beam radius (important for the 400 MHz cavity), dependence on the settings of bunching voltages (V_1 and ratio V_2/V_1) and, most important, the asymmetry in the bunching arising from any effective phase errors between the bunchers and also arising from defects in the phase response of the measuring system. The space charge effects, though important, are assumed to act symmetrically and not to alter the general conclusions relating to measured bunch shapes.

Modulation with the Double Drift Harmonic Buncher (DDHB)

The bunching possibilities of the DDHB are greater than those of a single buncher, but at the same time the adjustment is more complex. As the quality of bunching depends critically on the precision of the setting of bunching parameters, the modulation process with the DDHB will be first studied analytically. Although this analysis does not have a strict quantitative significance (the correct buncher settings have been found in Ref. 1 by optimization routines including space charge), it will nevertheless reveal the influence of various parameters on the bunch shape and be useful for comparisons during the study of bunch measurements.

Applying the usual bunching theory to the case of a DDHB, we can establish an expression which links the phase of a particle at the position of observation (in our case the position of the broad-band probe) to the phase at the first buncher B1 (see Fig. 1):

$$\phi_3 = \phi_1 - (\psi_{12}+\psi_{23})V_{10}T_1(r_1)\sin\phi_1 + \psi_{23}V_{20}T_2(r_2) \times \sin\{2[\phi_1-\psi_{12}V_{10}T_1(r_1)\sin\phi_1+\delta]\} .$$

The meaning of the various symbols is as follows (see also Fig. 1):

$$\psi_{12} = \frac{\pi}{\beta\lambda}\frac{e}{W}d_{12} , \qquad \psi_{23} = \frac{\pi}{\beta\lambda}\frac{e}{W}d_{2L}$$

$$\left.\begin{aligned} T_1(r_1) &= T_{10}\left[1+\left(\frac{\pi}{\beta\lambda}\right)^2 r_1^2\right] \\ T_2(r_2) &= T_{20}\left[1+\left(\frac{2\pi}{\beta\lambda}\right)^2 r_2^2\right] \end{aligned}\right\} \text{transit time factors.}$$

with W = kinetic energy of proton and λ = free space wavelength of the fundamental frequency. After fixing the geometry, W and λ, the phase ϕ_3 is a function of the remaining variables:

$$\phi_3 = f(\phi_1, V_{10}, V_{20}, r_1, r_2, \delta) \ .$$

Particles having the same ϕ_1 but different r_1 and r_2 at B1 and B2, respectively, will be bunched differently; this means that a tight bunching can be obtained only with beams which are narrow when passing through bunching gaps. Some examples of $\phi_3 = f(\phi_1)$ with V_{10}, V_{20}, r_1, r_2, and δ as parameters are shown in Fig. 2a. The three curves which are shown on each graph are due to the fact that the beam cross section was divided into three equal rings and the bunching of each ring computed separately.

A more interesting function than $\phi_3 = f(\phi_1)$ is the density distribution in the bunch, $i(\phi_3)$, which is the magnitude accessible to measurements and is defined by[2]:

$$i(\phi_3) = i_0 \sum \left| \frac{d\phi_1}{d\phi_3} \right| \ , \quad \phi_1 = f(\phi_3) \ ,$$

where i_0 represents the uniform longitudinal density of the unbunched beam, whilst $d\phi_1$ and $d\phi_3$ represent the phase extensions of the element of the beam under consideration at positions (1) and (3), respectively (see Fig. 1). The most convenient way of expressing $i(\phi_3)$ is as a Fourier series:

$$i(\phi_3) = a_0 + a_1 \cos \phi_3 + \ldots a_n \cos n\phi_3 + b_1 \sin \phi_3 + \ldots b_n \sin n\phi_3 \ ,$$

where the presence of the sin terms allows for asymmetries in the bunch. The Fourier coefficients are given by the usual integrals, which in the case of DDHB have to be evaluated numerically. To obtain more realistic bunch densities, the beam cross section at B1 and B2 is divided into three rings with equal population and the coefficients obtained as arithmetic averages

$$a'_m = \frac{a_{m1}+a_{m2}+a_{m3}}{3} \ ,$$

where a_{mi} corresponds to the i^{th} ring of the cross section. The same applies for b_m. It is interesting to compare the characteristic bunch densities $i(\phi_3)$ given in Fig. 2b with the familiar ones obtained with a single buncher. It can be seen that with DDHB it is possible to obtain two or more peaks of the curve $i(\phi_3)$. The ripple seen on this and other undamped waveforms arises from cut-off of the summation at n = 25. Unless $\delta \neq 0$, the curve is always symmetric about its centre, which is very important when measuring the correct phase setting between V_1 and V_2.

When making real-time bunch measurements, it is usual to display the bunch shape on an oscilloscope. Owing to the finite bandwidth of the measuring device, the higher Fourier coefficients will be damped and the original density curve changed (smoothed). If the frequency characteristics of the system are known, appropriate corrections can be introduced when interpreting the displayed bunch densities; the situation is particularly delicate when frequency-dependent phase shifts occur, causing asymmetries in the displayed curves even for $\delta = 0$. In Fig. 3 we show density curves obtained with single and double bunchers for various frequency damping and phase shift parameters.

The bandpass characteristic used is constant up to harmonic number n_1, then cutting off as a Gaussian defined by the 3 dB point at harmonic number n_2.

To first order we have assumed a phase shift of the n^{th} harmonic relative to the fundamental one given by

$$\theta_n = \arctan \left[(n-1)\theta \right] \ ,$$

where for both effects we aim to fit the parameters n_1, n_2 and θ to measured curves.

A more complete analysis treating the bunching gap as having finite thickness shows that there is an intrinsic asymmetry in the process even for a single buncher. For energy modulations $V_0T/W \leq 5\%$ we neglect these effects ($< 1^\circ$ shifts and $< 1\%$ asymmetry in ΔW). For an efficient adjustment of the bunching parameters, the beam size at the gaps has to be known and controlled, as larger beams cause an unnecessary widening of the bunch shape. A similar effect is caused also by increasing the ratio of bunched voltages V_{20}/V_{10}, as shown in Fig. 4.

Description of the Measuring System

The improvements described below were mainly intended to reduce the difficulties of observation of fast transients which previously have been a serious discouragement when using the 'fast probes' on operational linacs.

Broad-band Detector

The design of the broad-band detector profited from the experience gained with the one described previously[2], and in particular some of the difficulties encountered in biasing and obtaining a good transit time have been tackled in a different way. For frequencies above 2 GHz the possible mismatches and other effects which distort the response have not been considered important as they will have little relative influence after attenuation by the transmission line and the available oscilloscopes.

The new probe head consists essentially of an asymmetric strip line tapered smoothly to a coaxial line. The beam passes through a (negatively) polarized grid in the outer conductor and is stopped in the inner conductor on a tungsten insert (Fig. 5). A 1 mm gap between the grid and the inner conductor is thus achieved, resulting in a good transit time factor. (For 750 keV protons, an ideal 1 mm gap leads to a -3 dB reduction at 5.3 GHz.) The characteristic impedance of 50 Ω is maintained over the entire length of the probe by means of step-by-step calculation of the capacity at each cross section.

Compared to the probe previously used, the present arrangement is much simpler mechanically and electrically as the line inner conductor requires no bias connection or decoupling components, these being transferred to the grid in the outer body

which is more robust and accessible. The grid is mounted directly on the decoupling capacitor (C = = 200 pF), which is a sandwich construction using a 0.5 mm plate insulated by 0.15 mm teflon foils. The cover plate of the capacitor carries a stainless-steel aperture used as a dump for particles outside the aperture of the grid, thus avoiding bombardment of the capacitor plate and teflon foil. Another grid in front of this protection aperture is used as a trap for back-streaming electrons, which is important if one wants to control or prevent beam neutralization.

The open-ended structure of the head ensures better pumping of the line, which diminishes the possibility of sparking between grid and inner conductor. (On the previous device, sparking was thought to be caused by increased pressure due to outgassing of the tungsten insert.) The end has been designed such that the 'round trip' time for reflected signals can be expected not to exceed 100 psec.

Broad-band Oscilloscopes

The scope generally used was the Tektronix 519 because of its easy manipulation and relatively large screen (useful area 54 × 18 cm^2). A GR-50/125 Ω adapter matched the cable to the scope impedance. The brightness of the CRT trace was just on the limit for single shots. Multiple triggering (pulse to pulse) was used to increase the total intensity for photographic recording.

An EG&G Type 2236 A scope with a KR 3-B TW-CRT was equipped with a faster horizontal sweep (of 5 nsec linear part) and trace intensifier (unblanking) circuit corresponding to 12 mm horizontal deflection. The useful bandwidth fell below the 2 GHz specification as a balun transformer 50 Ω coax/2 × 100 Ω balanced had to be used to match the signal to the vertical deflection system. This scope was used when the extra writing speed and bandwidth were considered essential.

Associated Electronics

The limiting factor (apart from the bandwidth) of high-speed oscilloscopes for real-time observation is the poor light output, especially on single-shot mode (or with low repetition rates).

For photographic recording, the superposition of several shots can improve the brightness of the CRT trace, and for visual observation the comparison of successive signals is easier if the image always appears at the same place on the screen. Both require a stable trigger of the horizontal deflection of the oscilloscope. The required stability is of the same order as the trace width of the CRT for a given horizontal deflection speed, i.e. 20 psec for a 0.1 mm trace and 2 nsec/cm horizontal deflection. For the frequency of the first buncher of 202.5 MHz, this would correspond to 1.5° stability in phase. This criterion is met with a specially developed gated prescalar using ECL III technology. The logic derives triggers from the 202.5 MHz RF at any precisely adjustable moment during the proton beam pulse. Multiple triggers during one proton beam pulse (50 to 200 μsec duration) are possible with this logic provided that the horizontal deflection repetition of the scope used allows it (about every 10 μsec for the T519). This facility requires a stable mean energy of particles during the beam pulse, as otherwise differences in time of flight between buncher and probe cause a phase shift of successive bunch displays, making their direct superposition impossible. The stable trigger makes the adjustment between the 202.5 MHz and 405 MHz RF phases easier.

In order to be able to use these facilities also for the EG&G scope, a new fast time base and appropriate unblanking circuit have been designed. A capacitor discharge delivers a 100 V linear part of 5 nsec (between 25 and 75%) of the slope to the horizontal deflection plates, and a Blumlein-line pulse generator a 170 V pulse of 10 nsec half-width and 6 nsec (10 to 90%) rise- and fall-time to the unblanking. The latter circuit permits appreciably higher photographic recording speeds than is possible with the T519 oscilloscope (for single sweep).

Bunch Measurements: Methods and Results

Bunch measurements with a DDHB are considerably more complex than with a single buncher because of the three main variables, V_{10}, V_{20}, and δ, and coupled variables, beam current, W, r_1, and r_2. In practice it will be difficult to obtain consistent pulse shapes from one run to the next merely by setting the above parameters, i.e. the waveforms have to be observed. It is assumed that the beam can be focused sufficiently well for r_1 and r_2 to be within acceptable limits and for the signal on the probe to be representative of the whole beam. By previous calculation of the buncher cavities and by calibration of the RF monitoring loops, we could be relatively certain (±5%) of absolute values of $V_{10}T_1$ and $V_{20}T_2$ (peak energy modulations) with a better precision for relative values. The measurement of phase between the 200 MHz and 400 MHz RF excitations could be made precisely (±1° at 200 MHz), but only relative to an arbitrary zero phase (depending on coaxial line lengths and on the pre-injector energy). Thus we had to adopt a systematic way of setting up the phase for each accelerator physics run by observation of the bunch waveforms, and this was the main concern in the measurements described here.

In Fig. 6 we show on the left the bunches produced by the 400 MHz buncher operating alone at its nominal excitation level. Each successive waveform is shifted in phase with respect to the 200 MHz bunch shown at the bottom, and this procedure allows us to set the phases between the bunchers to ∿ ±10° (when the 200 MHz bunch falls exactly between the 400 MHz bunches). On the right of Fig. 6 are shown the corresponding combined waveforms produced when both bunchers are operating, and the effect of phase shifts on the symmetry can be clearly seen. The fine adjustment of phase about this approximate setting was made by observation of the combined bunch shapes (Fig. 7) where we see distinct changes in form for phase shifts 2.5° at 200 MHz.

Note that the measurement is sufficiently sensitive to be used for our purpose, but the absolute settings can only be obtained after taking account of distortions introduced by the measuring system itself (compare, for example, the theoretical curves of Fig. 3 and the measured results of Fig. 6).

Discussion and Conclusions

The measurements described in this paper have been carried out in the frame of the study program connected with the construction of the new linac. The feasibility of adjusting the DDHB via measured bunch shape forms has been investigated and a satisfactory answer found; some useful operational experience with a DDHB has been obtained.

Within the assumptions made concerning bandwidth limitations, the measured bunch shapes conform to those expected by the theory. The measuring system is sufficiently sensitive to detect phase shifts of a few degrees. However, if the correct phase is to be determined in an absolute way, work still remains to be done in eliminating distortions introduced by the measuring system and finding appropriate corrections when interpreting distorted oscilloscope waveforms.

Another important parameter is the beam diameter at the DDHB. In fact, in the new 750 keV beam transport, a beam profile measurement is foreseen just in front of the DDHB, and between the 200 MHz and 400 MHz bunchers a quadrupole is inserted for fine focusing adjustments.

In conclusion we must admit that as far as the bunching efficiency was concerned our present measuring method had a limited quantitative significance at 500 keV. However, when we can accelerate in the linac, the planned measurements at 10 MeV will help us to calibrate our (improved) observations at 750 keV and make them more useful in an absolute sense.

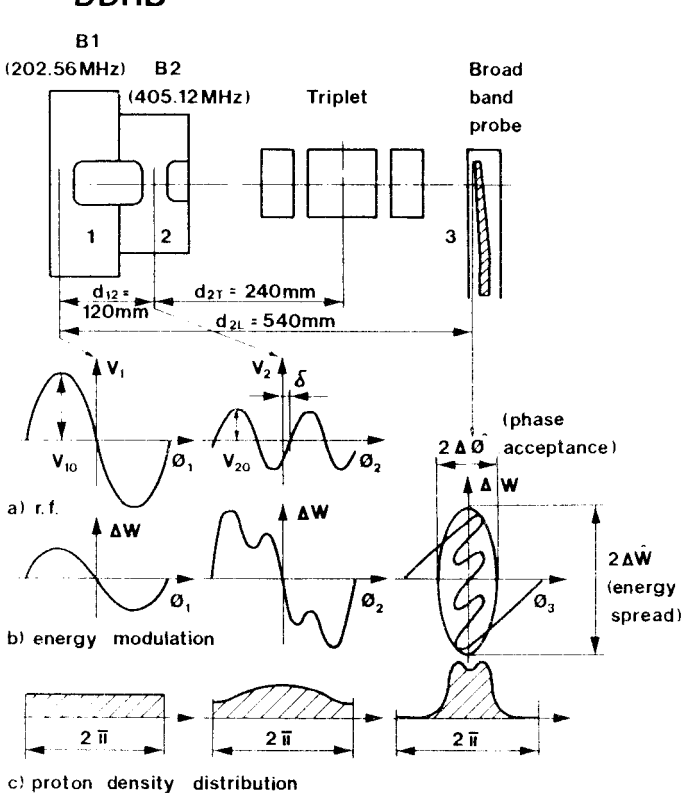

Fig. 1 Experimental DDHB system and its typical bunching curves

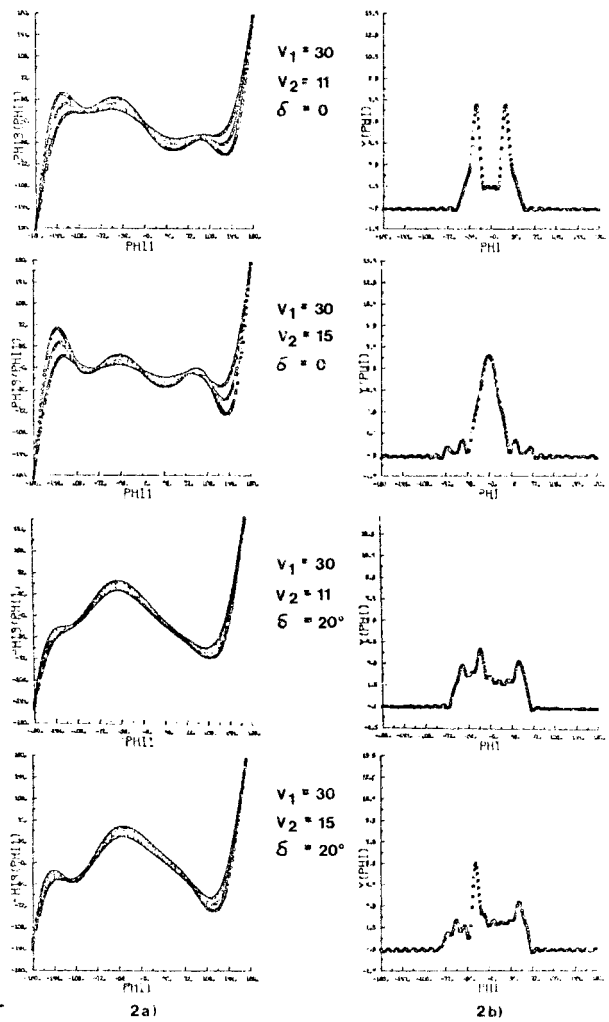

Fig. 2 Modulation curves (2a) and bunch densities (2b) for various settings of DDHB

Acknowledgements

A program of measurements involving an accelerator (be it only 500 keV energy) cannot succeed without the help of colleagues in many disciplines. We would particularly like to acknowledge the invaluable supporting work with source and 500 keV preaccelerator, with the two (phase locked) RF systems, with mechanical design, fabrication and installation, and finally with computation and display of results.

References

1) B. Bru and M. Weiss : Design of the low-energy beam transport system for the new 50 MeV linac, CERN/MPS/LIN 74-1 (1974).

2) L.R. Evans and D.J. Warner, Real-time measurements of proton bunch form, CERN/MPS/LIN 72-6 (1972).

3) J. Knott and M. Weiss, Review of results from the 500 keV measuring programme, CERN/MPS/LIN-Note 75-14 (1975).

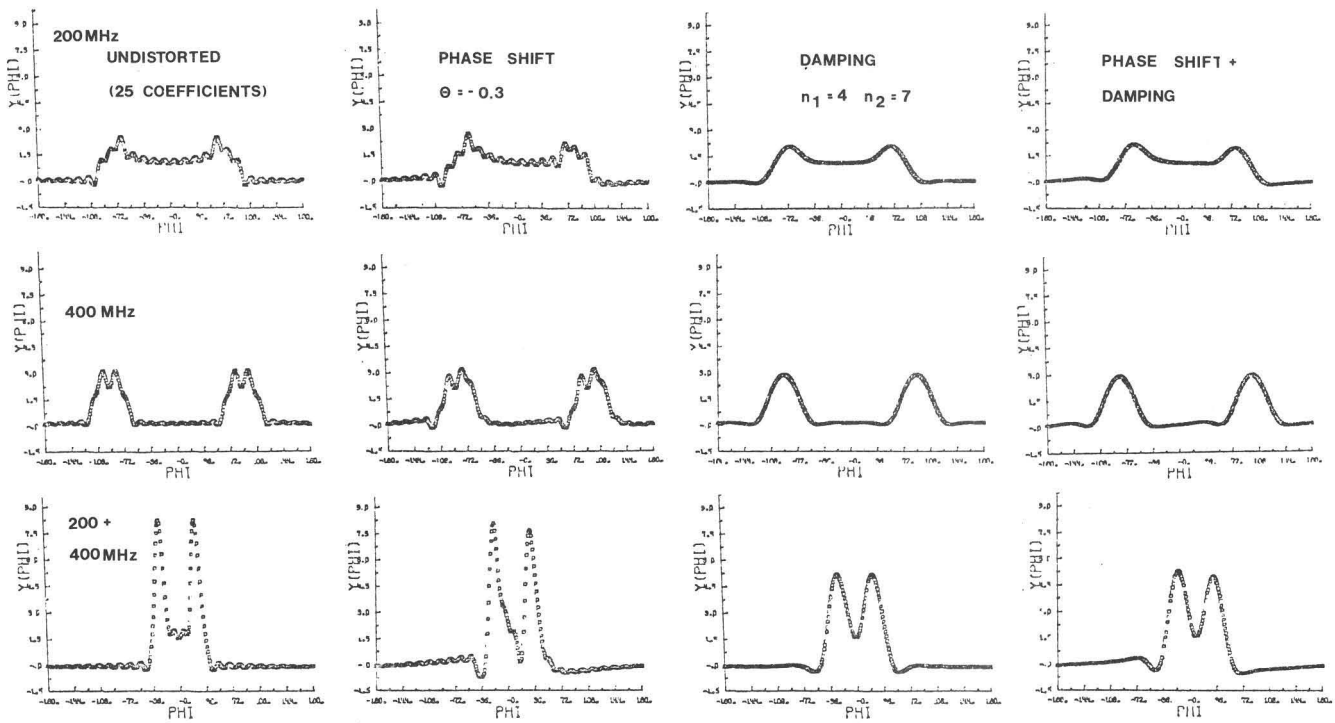

Fig. 3 Distortions in displayed bunch densities due to imperfections in the measuring system

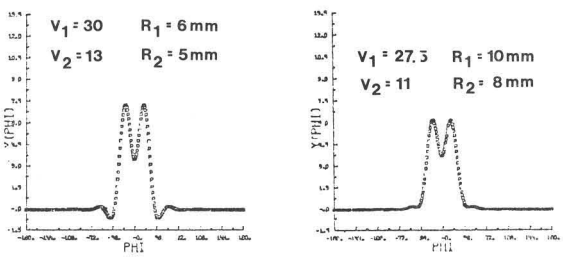

Fig. 4 Bunch densities as function of beam radii and buncher voltages

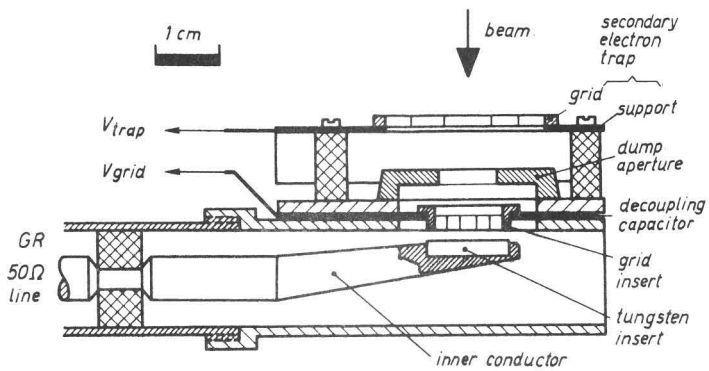

Fig. 5 Schematic drawing of the broad-band probe ▶

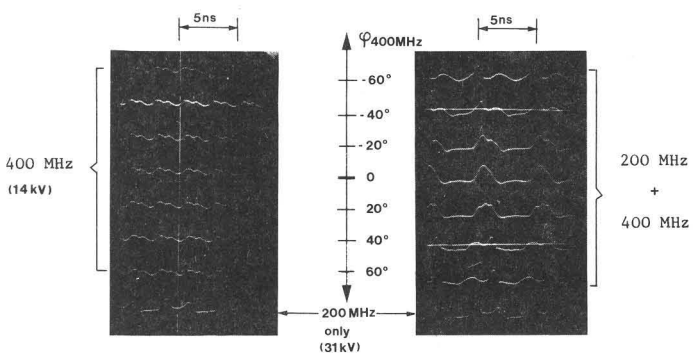

Fig. 6 Procedure for initial adjustment of DDHB

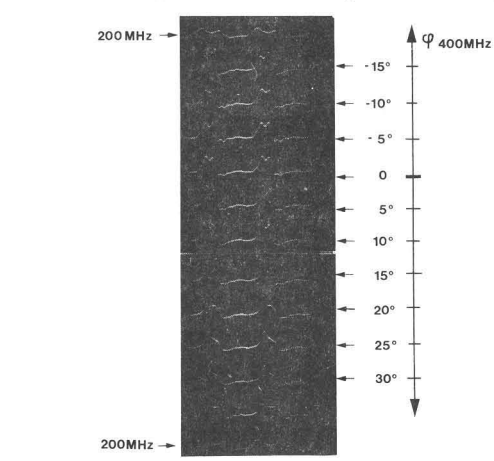

Fig. 7 Fine adjustment of DDHB